The Journal of Chemical Physics ARTICLE scitation.org/journal/jcp

Competition between ring-puckering and ring-opening excited state reactions exemplified on 5H-furan-2-one and derivatives

Cite as: J. Chem. Phys. 152, 064301 (2020); doi: 10.1063/1.5129366
Submitted: 27 September 2019 • Accepted: 19 January 2020 •
Published Online: 10 February 2020

Oliver Schalk,[1,2] Joachim Galiana,[3,4] Ting Geng,[1] Tobias L. Larsson,[3] Richard D. Thomas,[1] Ignacio Fdez. Galván,[3,5] Tony Hansson,[1] and Morgane Vacher[3,6,a)]

AFFILIATIONS

[1]Department of Physics, AlbaNova University Center, Stockholm University, 106 91 Stockholm, Sweden
[2]Department of Chemistry, University of Copenhagen, Universitetsparken 5, DK-2100 Copenhagen, Denmark
[3]Department of Chemistry–Ångström Laboratory, Uppsala University, P.O. Box 538, SE-751 21 Uppsala, Sweden
[4]Department of Chemistry, École normale supérieure de Lyon, 69342 Lyon, France
[5]Department of Chemistry–BMC, Uppsala University, P.O. Box 576, SE-751 23 Uppsala, Sweden
[6]Laboratoire CEISAM - UMR CNRS 6230, Université de Nantes, 44300 Nantes, France

Note: This paper is part of the JCP Special Topic on Ultrafast Molecular Sciences by Femtosecond Photons and Electrons.
[a)]**Author to whom correspondence should be addressed:** morgane.vacher@univ-nantes.fr

ABSTRACT

The influence of ring-puckering on the light-induced ring-opening dynamics of heterocyclic compounds was studied on the sample 5-membered ring molecules γ-valerolactone and 5H-furan-2-one using time-resolved photoelectron spectroscopy and *ab initio* molecular dynamics simulations. In γ-valerolactone, ring-puckering is not a viable relaxation channel and the only available reaction pathway is ring-opening, which occurs within one vibrational period along the C—O bond. In 5H-furan-2-one, the C=C double bond in the ring allows for ring-puckering which slows down the ring-opening process by about 150 fs while only marginally reducing its quantum yield. This demonstrates that ring-puckering is an ultrafast process, which is directly accessible upon excitation and which spreads the excited state wave packet quickly enough to influence even the outcome of an otherwise expectedly direct ring-opening reaction.

I. INTRODUCTION

Ring-opening dynamics is one of the major relaxation processes upon photoexcitation of unsaturated organic ring molecules and the one that leads to the greatest change of the molecular structure. This can be used, e.g., for photo-switching,[1] and several biological processes are triggered by this type of dynamics, e.g., vitamin D synthesis.[2] In several molecules, ring-opening is rather efficient,[3–5] while in other systems, competitive reactions are dominant.[6] One of the major processes that can prevent an efficient ring-opening is ring-puckering. Ring-puckering occurs when a C=C double bond (or potentially a C=N double bond) is present in the ring. It causes the ring to deform and the hydrogen atoms attached to the C-atoms to move out of the ring plane. The reason for this behavior can be explained on the fundamental unit: ethylene.[7] In ethylene, $\pi\pi^*$ excitation promotes one electron from a bonding orbital to an antibonding orbital along the C=C double bond, which then formally becomes a single bond. This pushes the carbon atoms apart and forces the hydrogen atoms to rotate around the C—C bond, leading to a transient sp^3-hybridization and, as a consequence, to pyramidalization of one of the carbon atoms. In a ring molecule, these motions are sterically hindered and result in ring-puckering.

Ring-puckering dynamics are initiated directly after photoexcitation as a consequence of populating a π^* orbital. We note that the Franck–Condon geometry is a saddle point, i.e., a maximum with respect to the bond twist, on the excited state surface, so it is not a Franck—Condon active mode but, nevertheless, a

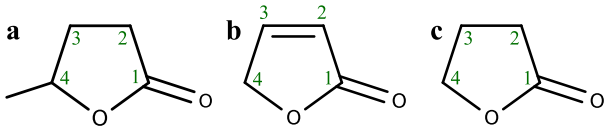

FIG. 1. Molecular structures of (a) γ-valerolactone, (b) furanone, and (c) γ-butyrolactone, with the numbering of the carbon atoms within the ring.

process that triggers immediately upon excitation. Depending on the shape of the excited state potential energy surface near the Franck–Condon geometry, ring-puckering can delay and block ring-opening dynamics, and thus reduces its quantum yield. In order to disentangle the dynamics and to understand the influence of ring-puckering, we examined a system where only ring-opening is accessible and ring-puckering is absent. We then compared the relaxation dynamics to those of a similar molecule where both ring-opening and ring-puckering are available.

Our reference system is γ-valerolactone [or 5-methyloxolan-2-one; see Fig. 1(a)], where ring-opening can occur at either of the C—O bonds, O—C_1 and O—C_4. In the reference molecule, the only double bond cannot undergo ring-puckering, as the bond is not between two ring atoms, or rotation, as the oxygen atom does not have any substituent. In comparison, 5H-furan-2-one [or 3-oxolene-2-one, further abbreviated as furanone; see Fig. 1(b)] has one extra C=C double bond within the ring, which allows for ring-puckering dynamics to occur. The same C—O ring-opening channels as in γ-valerolactone are available, and their combined quantum yield was reported to be >90% in the liquid phase upon excitation to the lowest lying $\pi\pi^*$ state.[8] The question we address here is if, and how much, ring-puckering influences the ring-opening dynamics. To do so, we have chosen time-resolved photoelectron spectroscopy, which allows following the potential energy surfaces as a function of delay time between the excitation photon and a probe photon. We have compared the experimental observations with *ab initio* molecular dynamics simulations to get a detailed understanding of the relevant processes. The *ab initio* simulations have also included γ-butyrolactone [or oxolan-2-one; see Fig. 1(c)] in order to estimate the influence of the extra methyl group that is added in 4-position to the ring in γ-valerolactone.

The remainder of the article is organized as follows: In Sec. II, the experimental and computational methods used are described. Both computational and experimental results are presented in Sec. III. A discussion is provided in Sec. IV while concluding remarks are offered in Sec. V.

II. METHODS

A. Experimental methods

Furanone (98%) and γ-valerolactone (99%) were purchased from Sigma-Aldrich and used without further purification.

Our magnetic bottle type photoelectron spectrometer and the other experimental conditions were identical to those described previously.[9,10] We used 200 nm for the pump and 267 nm for the probe pulses at integrated energies of 400 nJ/pulse and 2 μJ/pulse, respectively. The cross correlation in the experimental chamber was measured to be 160 ± 10 fs by utilizing the non-resonant signal of xenon, which also served as an energy calibration. The samples were introduced into the interaction region by evaporation through a gas needle and did not show any trace of cluster formation. At each time delay, the measured pump–probe signal was corrected by subtracting the background signals due to pump and probe laser pulses alone. The datasets consist of more than 20 runs where data were collected from 8000/1500/1500 laser shots for pump–probe/pump only/probe only at each time delay.

B. Data fitting

In order to extract more detailed information, the photoelectron spectra were fitted with a Levenberg–Marquart 2D global fitting scheme,[11] expressed as

$$S(E,\Delta t) = \sum_i A_i(E) P_i(\Delta t) \otimes g(\Delta t), \tag{1}$$

where $A_i(E)$ is the decay associated spectrum (DAS) of the channel i, which has a time-dependent population $P_i(\Delta t)$, expressed in terms of exponential functions $\exp(-\Delta t/\tau_i)$. Here, τ_i are the time constants of the respective decay processes, and $\Delta t = t_d - t_0$ is the time delay between the pump and probe pulses which overlap at time zero (t_0). Finally, $g(\Delta t)$ is the Gaussian cross correlation function obtained from fitting the time-dependence of the photoelectron spectrum of xenon.

Upon photoexcitation, large amplitude nuclear motion may occur. This causes the photoelectron kinetic energies to decrease upon pump–probe delay, because of a decrease in the potential energy of the molecule in the excited state and a concomitant rise in the ionization potential. To quantify the resulting dynamics, time zero can be artificially used as a fitting parameter.[10,12,13] The time scale of the "time-zero shift" can often be used to account for the time a wavepacket needs to reach a conical intersection with a lower lying potential energy surface.[13,14] Similarly, the fitted time constants might be dependent on the photoelectron kinetic energy, E. This is because the wavepacket occupies various regions of the potential energy surface at different delay times. If two different processes happen and both cause an extended time-zero shift, the interpretation of the data can be ambiguous because the two shifts would overlap.

In our experiments, the uncertainty of the time-zero fit is ±10 fs in the one photon pump—one photon probe region, and ±15 fs in the two photon probe region. The time constants often have an error of ±20 fs or lower, when they are smaller than the cross correlation time. These uncertainties are conservative estimations and are larger than the errors provided by the fitting routine.

C. Computational methods

The electronic structure of the molecules of interest was studied using the complete active space self-consistent field (CASSCF)[15,16] method, state-averaging over the first three singlet states equally (S_0, S_1, and S_2). In γ-valerolactone and γ-butyrolactone, the active space used consisted of 10 electrons distributed in 8 orbitals: the two σ and two σ^* orbitals of the two C—O bonds within the ring, the π and π^* orbitals of the C=O bond, plus the lone-pair orbital of the (C—)O(—C) perpendicular to the ring plane and the lone-pair orbital of the O(=C) in the ring plane. In furanone, the

active space used consisted of 12 electrons in 10 orbitals: the two additional orbitals were the π and π^* of the C=C bond (Fig. S2 in the supplementary material). The relativistic core-correlated atomic natural orbital (ANO-RCC) basis set with polarized double-zeta contraction (ANO-RCC-VDZP)[17] and the atomic compact Cholesky decomposition (acCD)[18] were used. Transition dipole moments between the ground and the first two valence excited states were calculated with the restricted active space state interaction (RASSI) method.[19] The sensitivity of the results with respect to adding dynamic correlation was tested through second-order perturbation theory with the CASPT2 method[20] [with ionisation potential - electron affinity (IPEA) shift set to 0 and imaginary shift set to 0.1 hartree].

Non-adiabatic "on-the-fly" dynamics was performed using the surface hopping method with Tully's fewest switches algorithm,[21–23] in combination with CASSCF for the electronic structure. The nuclear motion was treated classically by numerically integrating Newton's equations of motion using the velocity Verlet algorithm. A time step of 20 a.u., i.e., about 0.48 fs, was used. All nuclear coordinates were taken into account. Non-adiabatic transitions among any of the three lowest-energy singlet states were included. The decoherence correction proposed by Granucci and Persico was used with a decay factor of 0.1 hartree.[24] The implementation of the above methods in the OpenMolcas package was used.[25,26] For each molecular system, 100 trajectories were initiated on the S_2 state which is the bright state (see Sec. III A) around the equilibrium structure of the electronic ground state. Both initial positions and momenta were sampled from a Wigner distribution[27] to mimic the vibrational ground state before photoexcitation; this was performed using the Newton-X package.[28]

III. RESULTS

In this section, we present first the results obtained in the simulations on all three molecules, γ-valerolactone, γ-butyrolactone, and furanone, and then the results obtained in the measurements on γ-valerolactone and furanone. This allows for a direct interpretation of the experimental observations using the understanding gained from the simulations.

A. Computational results

In this subsection, we present first the calculations of the excited states at the Franck–Condon geometry, then the non-adiabatic molecular dynamics simulations, and finally, a general analysis.

1. Excited states at the Franck-Condon geometry

Table I gathers the electronic excitation energies and the transition dipole moments computed at the Franck–Condon geometry at CASSCF and CASPT2 levels of theory. For all three molecules, S_1 has an $n \rightarrow \pi^*$ character and is a dark state, while S_2 has a $\pi \rightarrow \pi^*$ character and is a bright state. The excitation energies for γ-butyrolactone and γ-valerolactone are very close at both CASSCF and CASPT2 levels of theory, demonstrating that the methyl group has no significant effect on the electronic structure of the molecules at the Franck–Condon geometry. The excitation energies for furanone are about 0.7 eV–1.3 eV lower than those for the two other molecules. This difference is mainly due to the delocalized π-system caused by the additional C=C double bond. The dynamic correlation energy calculated with CASPT2 is larger for the S_2 state than that for the S_1 state.

2. Ab initio molecular dynamics simulations

Ab initio molecular dynamics calculations have been performed to investigate the relaxation upon population of the S_2 bright state. We remind the reader that the energy of the pump photon is 6.2 eV. We note that experimental absorption spectra of both furanone[8] and γ-valerolactone[29] hint at fairly little excess energy upon excitation at 200 nm when considering a significant blue shift of the spectra in the gas phase as compared to the liquid phase.

Figure 2 shows the evolution of electronic populations of the ensemble of trajectories for all three molecules. We observe a fast non-adiabatic relaxation from S_2 to S_1 and S_0 states. The S_2 relaxation dynamics is similar for γ-valerolactone and γ-butyrolactone [Figs. 2(a) and 2(c)]: they show a fast population decrease of about 40% within the first 50 fs. The relaxation from S_1 to S_0 looks slower for γ-valerolactone than for γ-butyrolactone. One reason could be the inertia of the methyl group which slows down the relaxation dynamics. The S_2 relaxation dynamics in furanone is more gradual [Fig. 2(b)]. An exponential fit gives a decay time of about 170 fs.

TABLE I. Excitation energies and oscillator strengths of the S_1, and S_2 states for all three studied molecules, calculated at CASSCF/CASPT2 levels of theory at the Franck–Condon geometry.

Molecule	State	Energy (eV)	Oscillator strength
Furanone	S_0	0/0	...
	S_1 ($n \rightarrow \pi^*$)	5.22/5.02	8.48×10^{-4}/8.37×10^{-4}
	S_2 ($\pi \rightarrow \pi^*$)	7.18/6.35	1.07×10^{-1}/9.37×10^{-2}
γ-butyrolactone	S_0	0/0	...
	S_1 ($n \rightarrow \pi^*$)	5.94/5.85	1.57×10^{-3}/1.66×10^{-3}
	S_2 ($\pi \rightarrow \pi^*$)	9.02/7.65	2.88×10^{-1}/2.59×10^{-1}
γ-valerolactone	S_0	0/0	...
	S_1 ($n \rightarrow \pi^*$)	5.94/5.84	1.56×10^{-3}/1.66×10^{-3}
	S_2 ($\pi \rightarrow \pi^*$)	9.03/7.63	2.95×10^{-1}/2.64×10^{-1}

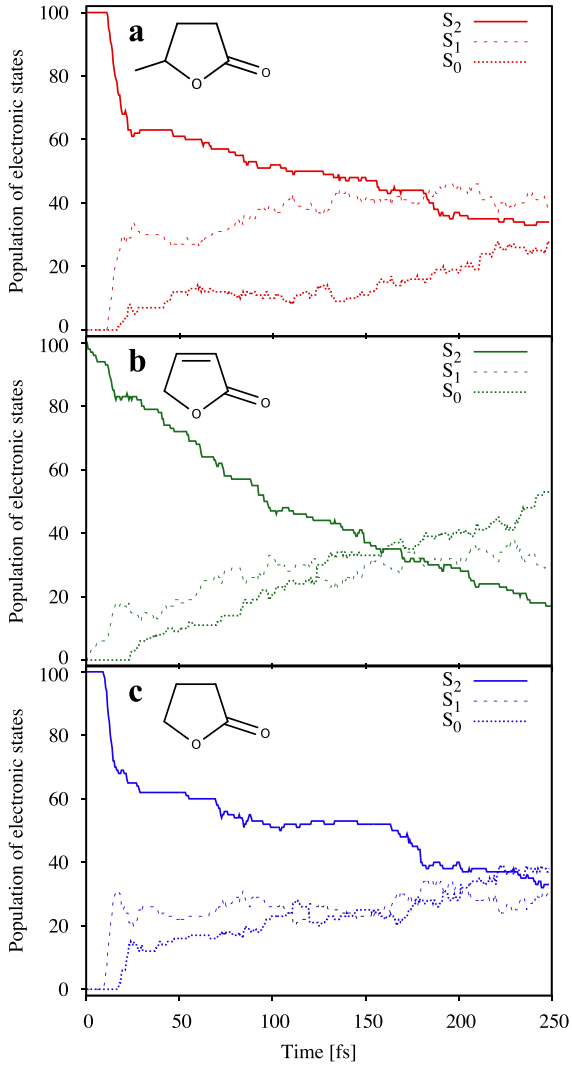

FIG. 2. Time evolution of the electronic populations of the ensemble of trajectories for (a) γ-valerolactone, (b) furanone, and (c) γ-butyrolactone.

After 600 fs of relaxation, three different products are observed (see Table II); dissociation is considered to occur when the distance between the carbon and the oxygen atom exceeds 3.2 Å, which is the sum of the carbon and oxygen van der Waals radii. (i) Ring-opening along the O—C_1 bond is found to be the main relaxation pathway for all three molecules. It represents >95% in both γ-valerolactone and γ-butyrolactone, and 85% in furanone, which is in good agreement with the liquid phase experiments of Murdock and co-workers.[8] (ii) Ring-opening along the O—C_4 bond is also observed in all three molecules, but only in a small number of trajectories (<5%). (iii) In furanone, a third channel is the non-adiabatic relaxation without bond cleavage. It amounts to 13% of the trajectories.

TABLE II. Number of trajectories with a first dissociation along O—C_4, O—C_1, or without any dissociation after 600 fs.

Molecule	O—C_4	O—C_1	Not dissociated
Furanone	2	85	13
γ-butyrolactone	4	96	0
γ-valerolactone	1	99	0

Figure 3 shows the number of trajectories dissociated along the O—C_1 bond as a function of time. For γ-valerolactone and γ-butyrolactone, almost all trajectories dissociate at approximately the same time and in less than 50 fs, which suggests an instant motion along the dissociation pathway upon excitation. About 60% of the trajectories dissociate adiabatically on S_2, while the remaining 40% undergo a non-adiabatic transition to either S_1 or S_0 [Figs. 2(a) and 2(c)]. Such splitting of the wavepacket was observed earlier, e.g., for furan.[30] In furanone, on the contrary, the ring-opening proceeds distinctively slower. It starts approximately 40 fs after excitation, and the dissociation curve can be well fitted by a monoexponential function with a time constant of 140 fs. It is noted that the splitting of the wavepacket between the different electronic states along the ring-opening pathway could not be extracted directly for furanone because the trajectories can relax non-adiabatically before the ring-opening process. For all three molecules, subsequent dynamics after ring-opening (including epoxidation[8] and CO elimination) are discussed in the supplementary material.

The delay of the ring-opening in furanone can be explained with ring-puckering motions that take place directly after excitation of the molecule and that allow the molecule to explore other regions of the potential energy surface of the excited states before undergoing ring-opening. This is not possible in the other two molecules. Figure 4 shows the dynamics of relevant nuclear coordinates and electronic state energies along a representative trajectory. Ring-opening along the O—C_1 bond begins shortly after 150 fs. Before then, we clearly see large oscillations in the HC_2C_3H dihedral angle [Fig. 4(a)] and bond alternation along the C=C—C=O chain [Fig. 4(b)]; ring-puckering motion, thus, takes place initially, postponing the ring-opening reaction. We also see that while opening, this trajectory decays non-adiabatically to S_1 and further to S_0 [Fig. 4(c)]. In the supplementary material, Fig. S3 shows the

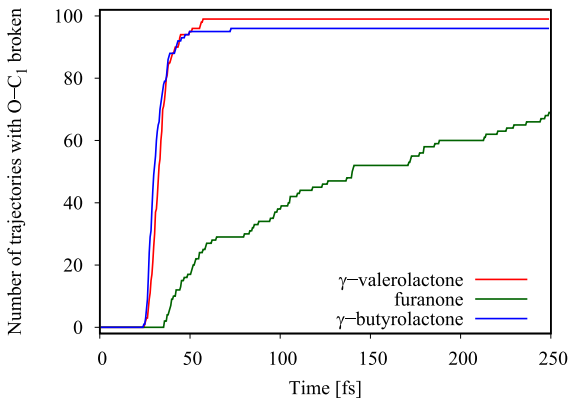

FIG. 3. Number of trajectories dissociated along the O—C_1 bond as a function of time for all three studied molecules.

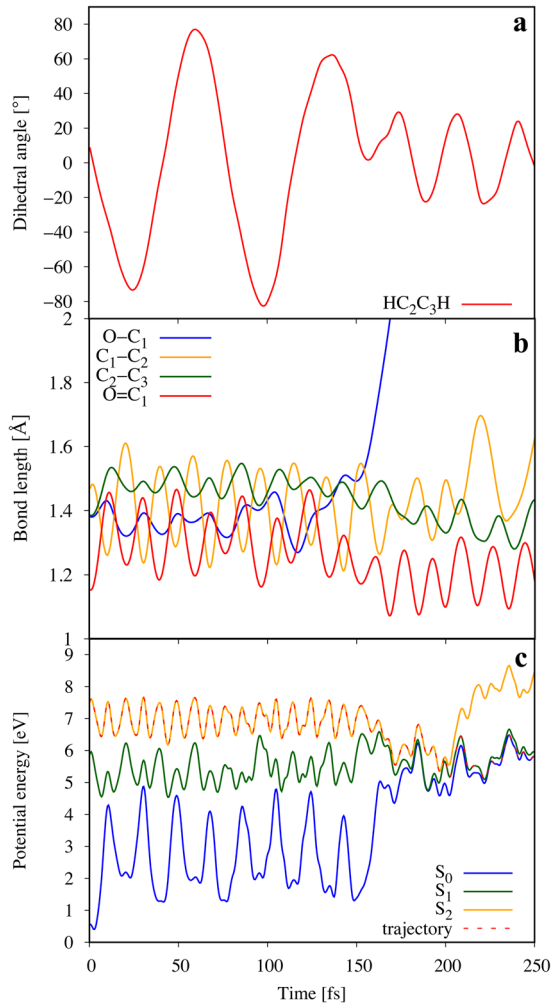

FIG. 4. Time evolution along one representative trajectory in furanone: (a) HC_2C_3H dihedral angle, (b) relevant bond lengths, and (c) potential energies of the three lowest-energy states and of the trajectory.

dynamics along another representative trajectory which undergoes ring-puckering and then ring-opening along O—C_1, but does not decay non-adiabatically and stays on S_2.

3. Analysis of the electronic state characters along the relaxation pathways

Further insight into the relaxation dynamics is gained by looking at the character of the excited states along the relaxation pathways. In the Franck–Condon region, the initial characters of the excited states are $\pi \rightarrow \pi^*$ for S_2 and $n \rightarrow \pi^*$ for S_1 for all three molecules. The π orbital actually mixes with the lone-pair orbital on the oxygen atom orthogonal to the ring plane (see Fig. S1): it will be referred to as $\pi/n_\perp$ in the following Sec. IV. The lone-pair orbital n involved in S_1 is the lone-pair of the carbonyl oxygen within the ring plane and mixes with the σ orbital of the C—O_1 bond (see Fig. S1): it will be referred to as $n_\parallel/\sigma$ in the following discussion.

During ring-puckering motions, the characters of the excited states are conserved (Fig. 5, left side). Along the ring-opening relaxation pathway toward O—C_1 dissociation, the excited states get close in energy, they interact, and their character changes. At the intersection between S_2 and S_1, the characters of the two excitations $\pi/n_\perp \rightarrow \pi^*$ and $n_\parallel/\sigma \rightarrow \pi^*$ mix. After the intersection, the S_2 state evolves toward a $\sigma \rightarrow \sigma^*$ excitation (probably influenced by a higher lying state getting close to S_2), while S_1 gets closer to S_0. At the intersection between S_1 and S_0, S_1 becomes $\pi/n_\perp \rightarrow \pi^*$ and S_0 becomes of $n_\parallel/\sigma \rightarrow \pi^*$ character (note that the ring-opened molecule has a biradical character, where the radical at the carbon atom is stabilized through the neighboring oxygen atom). Due to the dissociation, the σ and σ^* orbitals decompose into two $2p$ orbitals. The $n_\perp$ orbital which was initially mixed with a π orbital is referred to as a $2p$ orbital at the end of the pathway (Fig. 5, right side). Thus, in terms of excitations, the dissociation and ring-opening reaction occur with the excitation of an electron from a σ orbital (to a σ^* orbital if the trajectory stays on S_2 or to a π^* orbital if the trajectory decays onto S_1 or S_0).

As discussed above, a minor relaxation pathway is the O—C_4 dissociation. This relaxation pathway is analogous to O—C_1 dissociation in terms of relative energies of states. However, the characters of the excitations during and at the end of the relaxation process are different. For the ring-opening reaction along the O—C_1 bond, the electrons are excited from a σ-like orbital to a π^* orbital. However, bond cleavage along the O—C_4 bond requires an excitation to the σ^* orbital of the dissociating bond, probably making the process less favorable (see Fig. S4).

B. Experimental results

In this section, we present the experimental results of the dynamics probed by photoelectron spectroscopy. Time-resolved photoelectron spectra of γ-valerolactone and furanone are shown in Figs. 6 and 7, respectively. One pump photon and one probe photon deliver 6.2 eV + 4.65 eV = 10.85 eV total energy. For γ-valerolactone, the ionization threshold was found at 9.98 ± 0.05 eV. Based on this result, one expects the one photon pump, one photon probe [1, 1′] cutoff at 10.85 eV–9.98 eV = 0.87 eV.[31] This is in good agreement with our experimental value of 0.82 eV (Fig. 6). The adiabatic/vertical ionization potentials of furanone are

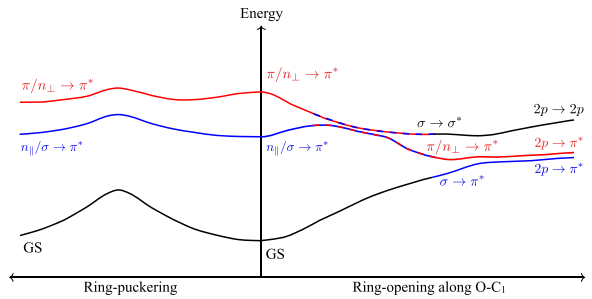

FIG. 5. Characters of the electronic states along the ring-puckering and (O—C_1) ring-opening pathways. The potential energy curves are based on relaxed scans performed in furanone, minimizing the S_0 state energy, of (left) the HC_2C_3H dihedral angle and (right) the O—C_1 bond length.

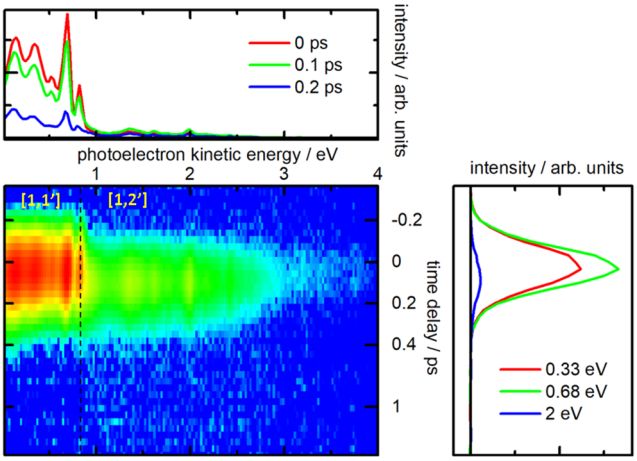

FIG. 6. Time-resolved photoelectron spectra of γ-valerolactone upon excitation with 200 nm photons and probe with 267 nm photons. The vertical dashed line indicates the frontier between [1, 1′] photoionization and [1, 2′] photoionization (see the text for details).

10.19 eV/10.57 eV,[32] respectively. Consequently, the [1, 1′] cutoff is at 10.85 eV–10.19 eV = 0.66 eV, which agrees with the first intense band of the time-resolved photoelectron spectrum in Fig. 7. A calculation of the vertical ionization potential of γ-valerolactone and furanone at the IP-CCSD/aug-cc-pVDZ level of theory revealed values of 10.53 eV and 10.43 eV, respectively, which suggests that the ionization potentials are not far apart. This agrees with the time-resolved photoelectron spectra, where the most intense peaks of both molecules are in the same energetic region. The photoelectron spectrum in the [1, 1′] energy region resembles the He(I) photoelectron spectrum for furanone,[32] which can be interpreted in that the molecule does not show any major rearrangements and ionization occurs from the initially excited state. For γ-valerolactone, the He(I) photoelectron spectrum is not known but the structure of the spectrum indicates a similar behavior. In the energy region above the [1, 1′] energy cutoff, the signal originates from a one photon pump–two photon probe signal. As a consequence, this signal is less intense. However, the observed signal reaches from regions further down on the potential energy surface because more total energy is available for photoionization.

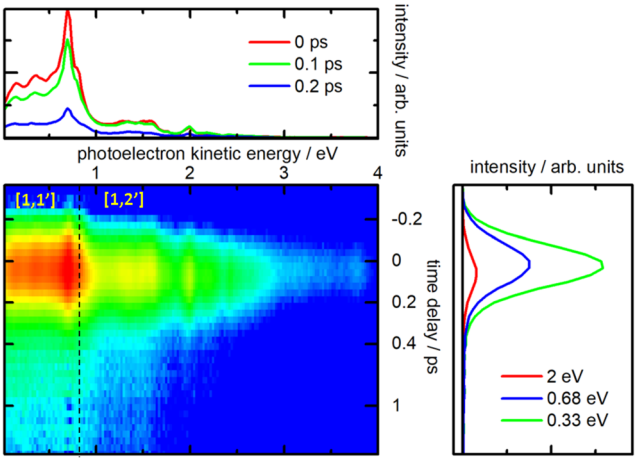

FIG. 7. Time-resolved photoelectron spectra of furanone upon excitation with 200 nm photons and probe with 267 nm photons. The vertical dashed line indicates the frontier between [1, 1′] photoionization and [1, 2′] photoionization (see the text for details).

The time-resolved photoelectron spectrum of γ-valerolactone can be fitted with a monoexponential decay function of (60 ± 20) fs and a time-zero shift in both the [1, 1′] and the [1, 2′] region. In the [1, 2′] region, the shift extends to (65 ± 10) fs (see Fig. 8 and Sec. II B for more information on this type of plot). The maximal time shift extends over more than 1 eV which suggests that the maximal shift is observed in our data. The process causing this shift can be assigned to the O—C_1 ring-opening reaction in γ-valerolactone because it is the only significant process in this molecule. The shifting time is slightly longer than the ring-opening process time scale found in our simulations, but the absence of any other time constants (i.e., any other relaxation process) agrees well with theory.

The time-resolved photoelectron spectrum of furanone is more complex. Fitting requires two time constants of (20 ± 10) fs and (200 ± 40) fs plus a time-zero shift, which extends to 40 fs in the [1, 2′] region. The corresponding DAS can be found in the supplementary material. When comparing the time-zero shifts of furanone and γ-valerolactone, one observes that the shift increases in the energy interval between 3.5 eV and 2 eV electron kinetic energy, but does not increase further as observed in γ-valerolactone. One possible interpretation is that the shift is not, or not only, caused by the ring-opening dynamics, but rather is governed by ring-puckering motion. This is in agreement with the theoretical results, where an incubation time of 40 fs was observed, which is needed for the molecules to open the ring. The total excited state dynamics of furanone is thus described by the second time constant of 200 fs, which can be assigned primarily to the ring-opening dynamics, albeit from a ring-puckered geometry; physically, it can be interpreted as the average delay of ring-opening caused by ring-puckering. This time constant is also in good agreement with the 140 fs time constant of the ring-opening dynamics obtained in the simulations.

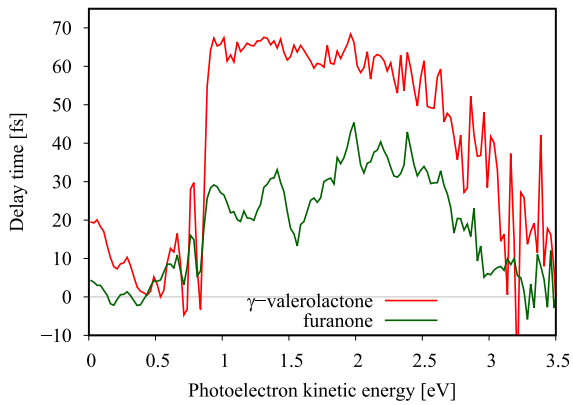

FIG. 8. Delay of the onset of the photoelectron signal ("time-zero shift") for furanone (green) and γ-valerolactone (red). See the text in Sec. II B for details.

IV. DISCUSSION

We have studied experimentally using time-resolved photoelectron spectroscopy and theoretically using *ab initio* molecular dynamics simulations the relaxation of furanone and lactones upon excitation of the low-lying $\pi\pi^*$ state (the S_2 state). In the studied lactones, γ-valerolactone and γ-butyrolactone, ring-opening along the O—C_1 bond is the major relaxation pathway. It occurs in approximately 50 fs. The additional methyl group in γ-valerolactone compared to γ-butyrolactone has no significant effect according to our simulations. In furanone, a competing relaxation pathway is ring-puckering, caused by the additional C=C present in the molecular ring. This process is responsible for spreading the wavepacket and thereby delaying the ring-opening relaxation reaction by about 150 fs. Ring-puckering also slightly decreases the yield of ring-opening since some part of the wavepacket decays non-adiabatically via ring-puckering only. It is also noted that in all three studied molecules, a minor relaxation pathway is ring-opening along the O—C_4 bond. The branching ratio between O—C_1 and O—C_4 ring-opening channels does not seem to be affected by the presence of the extra C=C double bond within the ring in furanone.

Setting the present study in a larger context, ring-opening and ring-puckering dynamics have been discussed for many five-membered heterocyclic systems. In furan derivatives, ring-opening supposedly occurs from a ring-puckered geometry[33] and the quantum yields of ring-opening and non-adiabatic decay through a ring-puckered structure are not yet determined.[30] In fact, recent experiments provide ambiguous results.[34,35] Contrary to the furanone case, the dynamics in furan derivatives are thought to take place sub-100 fs;[30,33,36] this might indicate that the presence of ring-puckering does not slow down dynamics to the same degree as observed in furanone. An alternative interpretation could be that ring-opening cannot be reached after a certain amount of ring-puckering motions because the two channels would diverge. This was observed, e.g., for cyclohexa-1,3-diene.[4] In that molecule, the initial relaxation leads toward a conical intersection and then to a ring-opened molecule, hexatriene, along a bond alternation mode. If the region of high non-adiabaticity is crossed a few times without ring-opening, the dissociation reaction does not occur and all molecules that remain in the excited state decay non-adiabatically to the ground state without opening.

Thus, in general, the presence of ring-puckering can have different effects on the excited state ring-opening dynamics of molecules. (i) It is possible that ring-puckering exists but that the ring-opening process is so fast that the ring opens irrespective of other motions (e.g., isoxazole, unpublished data). (ii) In the present case, ring-opening can occur at any time while the molecule is in the excited state. However, the process is slowed down and an alternative relaxation path opens when ring-puckering is available. (iii) It is further possible that ring-puckering can close down ring-opening dynamics after the molecule remained for some time on the excited state (cyclohexa-1,3-diene; see above). This can occur, e.g., when two different local minima on the excited state exist or when the lack of velocity of the wavepacket through the region of the conical intersection renders non-adiabatic crossing improbable. In case (iii), the product distribution does not provide any insight into the speed of the different reaction channels as would be possible to deduce by classical reaction kinetics.[37] In furanone, we have an example of case (ii) as the molecule undergoes ring-opening even at long relaxation times. However, some part of the wavepacket does decay non-adiabatically without ring-opening, i.e., case (iii). The challenging question is whether it is possible to deduce rules that allow classifying the type of reaction based on the chemical compound under investigation by means of a simple model and to make predictions on how the reaction will develop.

V. CONCLUSIONS AND OUTLOOK

We studied the light-induced ring-opening dynamics of γ-valerolactone and 5H-furan-2-one using time-resolved photoelectron spectra and *ab initio* quantum dynamics calculations. We found that ring-puckering constitutes a competitive pathway to ring-opening, when it is available, as in 5H-furan-2-one. The quantum yield is in this case reduced by 13%, which might be considered minor, but is relevant if compounds were to be introduced into a synthetic pathway or a photoswitching device. The reduction in the quantum yield is also associated with a delay in the ring-opening reactions caused by the puckering motions, as observed by comparing the time scales in γ-valerolactone, where puckering is not available, and 5H-furan-2-one, where puckering can occur.

Future studies might aim at a detailed understanding of the dependence of quantum yields and reaction rate from the structure of the molecules, which will be crucial for the development of future compounds. Simulating the observable time-dependent photoelectron spectra would also help interpreting the experimental results.

SUPPLEMENTAL MATERIAL

See the supplementary material for measured decay associated spectra, active orbitals used for furanone, other representative trajectories, analysis of state character along the O—C_4 ring-opening pathway, and subsequent dynamics in all three molecules, including epoxidation and CO elimination reactions.

ACKNOWLEDGMENTS

We acknowledge the generous support and technical advice of Professor Dr. Raimund Feifel. This work was partly financed by the Swedish Research Council (VR), the Knut and Alice Wallenberg Foundation, and the Wenner-Gren Foundation. The simulations were performed using resources provided by the Swedish National Infrastructure for Computing (SNIC) at the UPPMAX center.

REFERENCES

[1] M. Irie, "Diarylethenes for memories and switches," Chem. Rev. **100**, 1685–1716 (2000).
[2] M. Holick, J. MacLaughlin, M. Clark, S. Holick, J. Potts, R. Anderson, I. Blank, J. Parrish, and P. Elias, "Photosynthesis of previtamin D_3 in human skin and the physiologic consequences," Science **210**, 203–205 (1980).
[3] J. Cao, "Photoinduced reactions of both 2-formyl-2h-azirine and isoxazole: A theoretical study based on electronic structure calculations and nonadiabatic dynamics simulations," J. Chem. Phys. **142**, 244302 (2015).
[4] O. Schalk, T. Geng, T. Thompson, N. Baluyot, R. D. Thomas, E. Tapavicza, and T. Hansson, "Cyclohexadiene revisited: A time-resolved photoelectron spectroscopy and *ab initio* study," J. Phys. Chem. A **120**, 2320–2329 (2016).

[5]T. J. A. Wolf, D. M. Sanchez, J. Yang, R. M. Parrish, J. P. F. Nunes, M. Centurion, R. Coffee, J. P. Cryan, M. Gühr, K. Hegazy, A. Kirrander, R. K. Li, J. Ruddock, X. Shen, T. Vecchione, S. P. Weathersby, P. M. Weber, K. Wilkin, H. Yong, Q. Zheng, X. J. Wang, M. P. Minitti, and T. J. Martínez, "The photochemical ring-opening of 1,3-cyclohexadiene imaged by ultrafast electron diffraction," Nat. Chem. **11**, 504–509 (2019).

[6]G. Wu, S. P. Neville, O. Schalk, T. Sekikawa, M. N. R. Ashfold, G. A. Worth, and A. Stolow, "Excited state non-adiabatic dynamics of pyrrole: A time-resolved photoelectron spectroscopy and quantum dynamics study," J. Chem. Phys. **142**, 074302 (2015).

[7]B. G. Levine and T. J. Martínez, "Isomerization through conical intersections," Annu. Rev. Phys. Chem. **58**, 613–634 (2007).

[8]D. Murdock, S. J. Harris, J. Luke, M. P. Grubb, A. J. Orr-Ewing, and M. N. R. Ashfold, "Transient UV pump–IR probe investigation of heterocyclic ring-opening dynamics in the solution phase: The role played by n^* states in the photoinduced reactions of thiophenone and furanone," Phys. Chem. Chem. Phys. **16**, 21271–21279 (2014).

[9]T. Kłoda, A. Matsuda, H. O. Karlsson, M. Elshakre, P. Linusson, J. H. D. Eland, R. Feifel, and T. Hansson, "Strong-field photoionization of O_2 at intermediate light intensity," Phys. Rev. A **82**, 033431 (2010).

[10]O. Schalk, M. Stenrup, T. Geng, R. Lindh, R. D. Thomas, R. Feifel, and T. Hansson, "Influence of alkoxy groups on the photoinduced dynamics of organic molecules exemplified on alkyl vinyl ethers," J. Phys. Chem. A **119**, 11105–11112 (2015).

[11]O. Schalk, A. E. Boguslavskiy, and A. Stolow, "Substituent effects on dynamics at conical intersections: Cyclopentadienes," J. Phys. Chem. A **114**, 4058–4064 (2010).

[12]O. Schalk, A. E. Boguslavskiy, A. Stolow, and M. S. Schuurman, "Through-bond interactions and the localization of excited-state dynamics," J. Am. Chem. Soc. **133**, 16451–16458 (2011).

[13]O. Schalk, M. S. Schuurman, G. Wu, P. Lang, M. Mucke, R. Feifel, and A. Stolow, "Internal conversion versus intersystem crossing: What drives the gas phase dynamics of cyclic α, β-enones?," J. Phys. Chem. A **118**, 2279–2287 (2014).

[14]T. J. A. Wolf, T. S. Kuhlman, O. Schalk, T. J. Martínez, K. B. Møller, A. Stolow, and A.-N. Unterreiner, "Hexamethylcyclopentadiene: Time-resolved photoelectron spectroscopy and *ab initio* multiple spawning simulations," Phys. Chem. Chem. Phys. **16**, 11770–11779 (2014).

[15]B. O. Roos, P. R. Taylor, and P. E. Siegbahn, "A complete active space SCF method (CASSCF) using a density matrix formulated super-CI approach," Chem. Phys. **48**, 157–173 (1980).

[16]B. O. Roos, "The complete active space self-consistent field method and its applications in electronic structure calculations," Adv. Chem. Phys. **69**, 399–446 (1987).

[17]B. O. Roos, R. Lindh, P.-Å. Malmqvist, V. Veryazov, and P.-O. Widmark, "Main group atoms and dimers studied with a new relativistic ANO basis set," J. Phys. Chem. A **108**, 2851–2858 (2004).

[18]F. Aquilante, L. Gagliardi, T. B. Pedersen, and R. Lindh, "Atomic Cholesky decompositions: A route to unbiased auxiliary basis sets for density fitting approximation with tunable accuracy and efficiency," J. Chem. Phys. **130**, 154107 (2009).

[19]P. Å. Malmqvist, B. O. Roos, and B. Schimmelpfennig, "The restricted active space (RAS) state interaction approach with spin–orbit coupling," Chem. Phys. Lett. **357**, 230–240 (2002).

[20]P. Å. Malmqvist, K. Pierloot, A. R. M. Shahi, C. J. Cramer, and L. Gagliardi, "The restricted active space followed by second-order perturbation theory method: Theory and application to the study of CuO_2 and Cu_2O_2 systems," J. Chem. Phys. **128**, 204109 (2008).

[21]J. C. Tully and R. K. Preston, "Trajectory surface hopping approach to nonadiabatic molecular collisions: The reaction of H^+ with D_2," J. Chem. Phys. **55**, 562–572 (1971).

[22]J. C. Tully, "Molecular dynamics with electronic transitions," J. Chem. Phys. **93**, 1061–1071 (1990).

[23]J. P. Malhado, M. J. Bearpark, and J. T. Hynes, "Non-adiabatic dynamics close to conical intersections and the surface hopping perspective," Front. Chem. **2**, 97 (2014).

[24]G. Granucci and M. Persico, "Critical appraisal of the fewest switches algorithm for surface hopping," J. Chem. Phys. **126**, 134114 (2007).

[25]OpenMolcas, version v18.09, tag 441-ge3cf8a6, https://gitlab.com/Molcas/OpenMolcas, 2018.

[26]I. Fdez. Galván, M. Vacher, A. Alavi, C. Angeli, F. Aquilante, J. Autschbach, J. J. Bao, S. I. Bokarev, N. A. Bogdanov, R. K. Carlson, L. F. Chibotaru, J. Creutzberg, N. Dattani, M. G. Delcey, S. S. Dong, A. Dreuw, L. Freitag, L. M. Frutos, L. Gagliardi, F. Gendron, A. Giussani, L. González, G. Grell, M. Guo, C. E. Hoyer, M. Johansson, S. Keller, S. Knecht, G. Kovačević, E. Källman, G. Li Manni, M. Lundberg, Y. Ma, S. Mai, J. P. Malhado, P. Å. Malmqvist, P. Marquetand, S. A. Mewes, J. Norell, M. Olivucci, M. Oppel, Q. M. Phung, K. Pierloot, F. Plasser, M. Reiher, A. M. Sand, I. Schapiro, P. Sharma, C. J. Stein, L. K. Sørensen, D. G. Truhlar, M. Ugandi, L. Ungur, A. Valentini, S. Vancoillie, V. Veryazov, O. Weser, T. A. Wesołowski, P.-O. Widmark, S. Wouters, A. Zech, J. P. Zobel, and R. Lindh, "OpenMolcas: From source code to insight," J. Chem. Theory Comput. **15**, 5925–5964 (2019).

[27]E. Wigner, "On the quantum correction for thermodynamic equilibrium," Phys. Rev. **40**, 749–759 (1932).

[28]M. Barbatti, G. Granucci, H. Lischka, M. Persico, and M. Ruckenbauer, NEWTON-X: A package for Newtonian dynamics close to the crossing seam, version 0.11b, www.univie.ac.at/newtonx, 2006.

[29]W. D. Closson, P. J. Orenski, and B. M. Goldschmidt, "Effect of conformation on the electronic absorption spectrum of the carboxylate group," J. Organ. Chem. **32**, 3160–3163 (1967).

[30]S. Oesterling, O. Schalk, T. Geng, R. D. Thomas, T. Hansson, and R. de Vivie-Riedle, "Substituent effects on the relaxation dynamics of furan, furfural and β-furfural: A combined theoretical and experimental approach," Phys. Chem. Chem. Phys. **19**, 2025–2035 (2017).

[31]J. Czekner, C. A. Taatjes, D. L. Osborn, and G. Meloni, "Absolute photoionization cross-sections of selected furanic and lactonic potential biofuels," Int. J. Mass Spectrom. **348**, 39–46 (2013).

[32]W. Dianxun, W. Dong, L. Sheng, and L. Ying, "He I photoelectron spectroscopic studies of the electronic structure of 2(3H) furanone and 2(5H) furanone," J. Electron Spectrosc. Relat. Phenom. **70**, 167–172 (1994).

[33]R. Spesyvtsev, T. Horio, Y.-I. Suzuki, and T. Suzuki, "Excited-state dynamics of furan studied by sub-20-fs time-resolved photoelectron imaging using 159-nm pulses," J. Chem. Phys. **143**, 014302 (2015).

[34]O. Schalk, T. Geng, T. Hansson, and R. D. Thomas, "The ring-opening channel and the influence of Rydberg states on the excited state dynamics of furan and its derivatives," J. Chem. Phys. **149**, 084303 (2018).

[35]S. Adachi, T. Schatteburg, A. Humeniuk, R. Mitrić, and T. Suzuki, "Probing ultrafast dynamics during and after passing through conical intersections," Phys. Chem. Chem. Phys. **21**, 13902–13905 (2019).

[36]T. Fuji, Y.-I. Suzuki, T. Horio, T. Suzuki, R. Mitrić, U. Werner, and V. Bonačić-Koutecký, "Ultrafast photodynamics of furan," J. Chem. Phys. **133**, 234303 (2010).

[37]P. L. Houston, *Chemical Kinetics and Reaction Dynamics* (Courier Corporation, 2012).